Geophysical Research Letters

RESEARCH LETTER
10.1029/2021GL096393

Threshold Conditions for the Shift Between Vegetated and Barebed Rivers

G. Calvani[1], C. Carbonari[1], and L. Solari[1]

[1]Department of Civil and Environmental Engineering, University of Florence, Florence, Italy

Key Points:

- Formulations for the threshold conditions between vegetated and barebed channel are derived
- Threshold conditions are mainly related to species-dependent characteristics
- Submerged plants are more vulnerable to removal than emergent as relative emergence reduces the threshold value

Correspondence to:

G. Calvani,
giulio.calvani@unifi.it

Citation:

Calvani, G., Carbonari, C., & Solari, L. (2022). Threshold conditions for the shift between vegetated and barebed rivers. *Geophysical Research Letters*, *49*, e2021GL096393. https://doi.org/10.1029/2021GL096393

Received 28 SEP 2021
Accepted 27 NOV 2021

Abstract Vegetation plays a fundamental role in riverine environments, by affecting both hydrodynamics and morphodynamics. At the same time, flow velocity and sediment scouring influence the decay of plants by uprooting. The balance among such interactions defines whether or not rivers are colonized by submerged or emergent vegetation. Previous studies focused on the shift between vegetated and barebed conditions through flume experiments or numerical simulations. Herein, we derive analytical formulations for the threshold in terms of flow velocity and Froude number, by accounting for the conditions of submergence. Both the formulations predict lower thresholds for submerged vegetation than emergent plants. Vegetation characteristics and flow regime variability play the major role in controlling the thresholds. The comparison of the proposed relationships to available data shows a good agreement. These results have important implications to understand bio-morphological changes induced by natural and human factors, as well as to design effective river restoration projects.

Plain Language Summary Fluvial systems are amongst the most biologically and economically important environments. The interactions between water, sediments, ecological components, as well as human interventions lead to the developments of different riverine habitats. In this work we refer to the presence or not of submerged plants, generally growing in water and emergent vegetation, generally riparian shrubs and trees growing on riverbanks. We provide simple formulations to discriminate conditions for which plant species may colonize and survive in a given fluvial environment. The critical conditions are derived in terms of the mean flow velocity and the Froude Number, a dimensionless quantity relating flow velocity to the water depth. We tested the proposed formulations against data from real rivers and highlighted that submerged vegetation shows lower values of the threshold quantities than emergent plants. Besides other factors, the analysis may explain why submerged plants are less common in large rivers and paves the way to understand the evolution of the riverine systems subject to climate change, colonization by invasive species and human interventions.

1. Introduction

The presence of vegetation in fluvial environments was widely studied during the last decades (Nepf, 2012; Solari et al., 2016; Wang et al., 2015, for a review). As part of the riverine habitat, plants have strong influence on hydrodynamics, by altering the flow field (Bennett et al., 2002) and providing additional flow drag (Aberle & Järvelä, 2013; Luhar & Nepf, 2013, among others), and on morphodynamics, by affecting threshold conditions for the incipient motion of sediment (Yang et al., 2016) and the sediment transport rate (Vargas-Luna et al., 2015; Västilä & Järvelä, 2018). Moreover, the presence of both submerged and emergent vegetation positively impacts the quality of the fluvial system (Dosskey et al., 2010, for a review). Additionally, recent studies demonstrate the influence of fluvial vegetation on the trapping of pollutant microplastics (Schreyers et al., 2021). At the same time, water flow and sediment transport affect vegetation growth, spread and decay through processes of burial (Pasquale et al., 2014) and uprooting (Edmaier et al., 2011, 2015). Furthermore, recent studies investigated the influence of sediment supply and channel dynamics on the altered growth of vegetation at a river-basin scale (Gran et al., 2015).

Vegetation dynamics in fluvial environments is typically modeled by the evolution in time and space of the plant density. The equation includes a growth term, whose general solution is represented by a logistic function (Camporeale & Ridolfi, 2006) and a decay term due to plant mortality induced by flow uprooting (Perona et al., 2014). Further terms can be included in the equation. These terms are usually represented by high-order space-derivatives of the plant density. For instance, D'Odorico et al. (2007) and Crouzy et al. (2016) proposed a diffusive term (i.e., the Laplacian $\Delta = \partial^2/\partial x^2 + \partial^2/\partial y^2$) to account for positive feedbacks between neighboring plants, later used

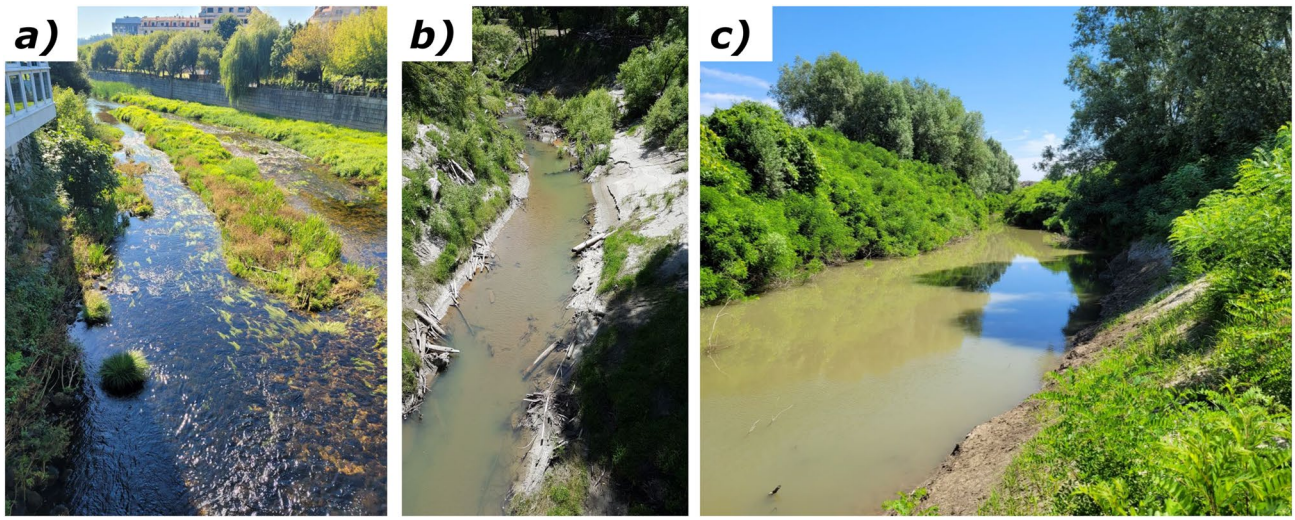

Figure 1. Riparian and submerged vegetation in rivers (pictures taken by the authors). (a) Downstream view of the Rio Umia in Caldas de Eris (ES) (coordinates 42°36′10.49″N 08°38′33.51″W) with submerged plants and grassy vegetation on the in-channel deposits (July 2021). (b) Upstream view of the Mangatokerau River near the confluence into the Hikuwai River (NZ) (coordinates 38°17′57.26″S 178°15′31.36″E) with young shrubs on the banks (December 2019). (c) Downstream view of the Secchia River near San Possidonio (IT) (coordinates 44°53′30.63″N 10°58′26.31″E) with mature bushes and trees on the banks (June 2021).

by Bärenbold et al. (2016) to perform a stability analysis of vegetated patches. Furthermore, Lejeune et al. (2002) involved a bi-Laplacian term (i.e., Δ^2) to investigate the dynamics of plants in arid landscapes.

While most of the research investigated the stability conditions for the emergence of vegetated patches, few studies focused on the thresholds for the shift between vegetated and barebed states (Figure 1). Bendix (1999) showed the influence of the unit stream power on riparian vegetation in the Piru and Sespe creeks (California, USA). However, they concluded that vegetation may even survive in regions subjected to high stream power. Bertoldi et al. (2014) numerically simulated the morphological evolution of the Magra River (Italy) by involving simple relations for vegetation dynamics and its effects on flow velocities and sediment transport. They found a range for the stream power, ω, where the shift towards barebed conditions occurred. Perona et al. (2012) carried out flume experiments with Avena sativa and found that the ratio between duration and intertime of flood plays a key role in the uprooting process. More recently, Bertagni et al. (2018) and Calvani, Perona, Zen et al. (2019) considered the dynamics of vegetation and variable flow discharges, mathematically simulated by a Compound Poisson Process. Similarly to Perona et al. (2012), they found that the flow variability (parametrized by c_v and β_p in Bertagni et al., 2018 and Calvani, Perona, Zen et al., 2019 respectively) determines the threshold between vegetated and unvegetated conditions.

In this work, we take into account the equation for vegetation dynamics at the steady state and derive simple relations for the critical conditions for which submerged and emergent plants are completely removed from the fluvial system (shift from vegetated to barebed conditions). Then, the proposed equations are tested against data available in literature and the comparison shows a good agreement. Additionally, the proposed formulations hint that the threshold values are mostly dependent on vegetation characteristics, thus suggesting that either plants adapted to live in a certain fluvial environment, or the fluvial system operates as a species selector. Besides the interest for river scientists, outcomes of our analysis have direct implications for practitioners to design restoration projects.

2. Mathematical Formulation

The dynamics of vegetation density is usually modeled by the sum of a growth term, a diffusive term mimicking the positive feedbacks among nearby plants (D'Odorico et al., 2007), and a decay term to account for plant removal due to flow drag acting on the submerged height of the plants (Perona et al., 2014). Previous studies considered that each process (growth, spread, decay) does not occur at the same time. For instance, the decay due to uprooting takes place during flood events only, while such high-flow conditions inhibit the growth process (Crouzy et al., 2016). Bärenbold et al. (2016) considered that plants grow for a period t_g, diffusion takes place

during a time t_D, and flow removal lasts t_d, over a total timescale $T = t_g + t_D + t_d$. Accordingly, the 1D equation for vegetation dynamics can be written as:

$$\frac{\partial \phi}{\partial t} = \alpha_g \phi (\phi_m - \phi) \frac{t_g}{T} + \alpha_D \Delta \phi \frac{t_D}{T} - \alpha_d \phi \min\{h_v, Y\} U^2 \frac{t_d}{T} \tag{1}$$

where ϕ is the spatial density of vegetation, t is time, ϕ_m is the carrying capacity, Y is the water depth, h_v is the plant height, U is the mean flow velocity, and α_g, α_D and α_d are the growth, diffusion and decay rate, respectively. The term $\min\{h_v, Y\}$ accounts for the effective height subjected to flow drag. We remark that the decay rate α_d depends on flow regime as well, while ϕ_m, α_D and α_g are species dependent only (Calvani, Perona, Schick, et al., 2019). To be consistent with the 1D formulation, the Laplacian operator in Equation 1 accounts for the spatial derivative in the longitudinal direction, only. In 2D models, the equation can be modified by replacing the longitudinal velocity U by the modulus of the flow velocity, $|\vec{V}|$ (Bärenbold et al., 2016), and by considering both the longitudinal and the transversal coordinates in the Laplacian term. At equilibrium, the left-hand side term (i.e., the time derivative) is null, as well as spatial derivative terms (e.g., Laplacian). In this condition, Equation 1 simplifies to:

$$\alpha_g \phi (\phi_m - \phi) t_g - \alpha_d \phi \min\{h_v, Y\} U^2 t_d = 0 \tag{2}$$

which is a quadratic equation in the variable ϕ. Bärenbold et al. (2016) already found that the problem admits a trivial solution $\phi_{0,2} = 0$, where the subscript 0 refers to equilibrium conditions. As such, no vegetation is never allowed to grow and establish. The non-trivial solution of Equation 2 reads:

$$\phi_{0,1} = \phi_m - \frac{\alpha_d t_d}{\alpha_g t_g} min\{h_v, Y\} U^2 \tag{3}$$

The form of Equation 3 suggests that the solution, $\phi_{0,1}$, may vanish (i.e., $\phi_{0,1} = 0$) according to the values of the parameters on the right-hand side. By arranging the terms, Equation 3 yields to the condition of the critical velocity U_c:

$$U_c = \begin{cases} U_v & \text{if } h_v \le Y \\ U_v \sqrt{h_v/Y} & \text{if } h_v > Y \end{cases} \tag{4}$$

with

$$U_v = \sqrt{\frac{\alpha_g}{\alpha_d} \frac{t_g}{t_d} \frac{\phi_m}{h_v}} \tag{5}$$

The critical velocity U_c represents the threshold value of mean flow velocity for the switch between vegetated ($U < U_c$) and barebed ($U \ge U_c$) conditions (Figure 2a). The ratio h_v/Y represents the relative emergence. By introducing the celerity $(g\ Y)^{1/2}$, where g is the acceleration due to gravity, Equation 4 can be made dimensionless, thus it reads:

$$Fr_c = \begin{cases} Fr_v \sqrt{h_v/Y} & \text{if } h_v \le Y \\ Fr_v\ h_v/Y & \text{if } h_v > Y \end{cases} \tag{6}$$

with

$$Fr_v = \frac{U_v}{\sqrt{g h_v}} = \sqrt{\frac{\alpha_g}{\alpha_d} \frac{t_g}{t_d} \frac{\phi_m}{g\ h_v^2}} \tag{7}$$

The quantity $Fr_c = U_c\ (g\ Y)^{-1/2}$ represents the critical Froude number for the establishment of vegetation (Figure 2b). Similarly to U_c, it turns out that vegetation can withstand flood events and may settle when the Froude number is lower than Fr_c. On the contrary, the riverbed remains unvegetated when the Froude number is

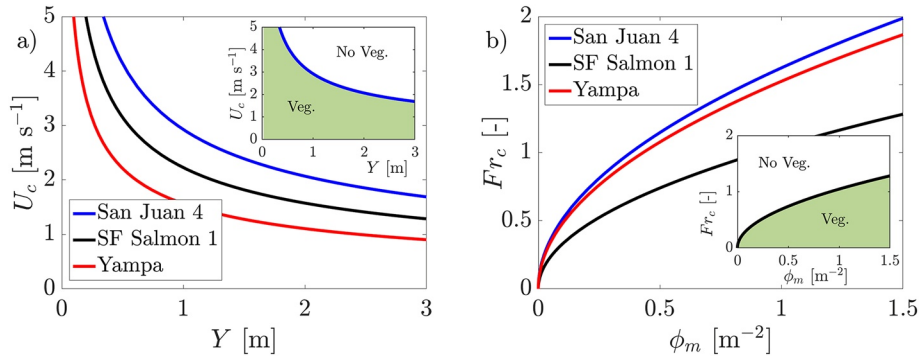

Figure 2. Threshold conditions for the establishment of vegetation for the San Juan River (reach 4, blue line), the SF Salmon River (reach 1, black line) and the Yampa River (red line). Vegetation and hydraulic parameters are taken from Table 1. (a) The critical velocity U_c versus water depth Y (Equation 4). Inset panel shows regions of vegetated and unvegetated conditions for the San Juan River (reach 4). (b) The critical Froude number Fr_c versus carrying capacity ϕ_m (Equation 6). Inset panel shows regions of vegetated and unvegetated conditions for the SF Salmon River (reach 1).

higher than the critical value. This result was graphically obtained by Bärenbold et al. (2016), while in this work we explicitly provide an analytical expression. For given characteristics and properties of the vegetation, both the Equations 4 and 6 show that the threshold variables admit a maximum in correspondence of emergent conditions. This is clearly highlighted by the presence of the term h_v/Y (i.e., the inverse of the submergence degree) which is always higher than one for emergent vegetation. In almost emergent conditions (i.e., $h_v = Y$), the thresholds U_c and Fr_c equal the quantities U_v and Fr_v, respectively. These critical values are mostly dependent on vegetation properties (i.e., species and growth stage), as shown by Equations 5 and 7.

3. Results

The graphical behavior of Equations 4 and 6 for plant in emergent conditions are plotted in Figures 2a and 2b, respectively. Interestingly, the curves show that the amplitude of vegetated regions depends on the critical variable. For instance, the formulation for threshold velocity (Equation 4) predicts a higher vegetated region (the area below the critical curve) for SF Salmon River (reach 1, black line in Figure 2a) than the Yampa River (red line in the same plot). Conversely, the formulation for the critical Froude number (Equation 6) indicates that the vegetated region is higher for the Yampa River (compare the regions below the black and red lines in Figure 2b).

We validate the proposed relationships for the critical velocity, U_c, and the critical Froude number, Fr_c, by comparing predicted values to the calculated thresholds for the rivers listed in Table 1. For the sake of comparison, we derive threshold values for the rivers in Table 1 by rearranging Equation 4 in Calvani, Perona, Schick, et al. (2019), a formula modeling the conditions for which plants disappear in vegetated channels with converging riverbanks. From such equation, by involving the Manning relation, one can obtain:

$$U_c^m = (k_s\, S)^{3/10}\left(G\left(\theta_s + q_s^{2/3}\right)\right)^{-3/20}\left(\phi_m \frac{\alpha_g\, t_g}{\alpha_d\, t_d}\right)^{7/20} \tag{8}$$

$$Fr_c^m = g^{-1/2} k_s^{33/40}\, S^{9/20}\left(G\left(\theta_s + q_s^{2/3}\right)\right)^{-3/80}\left(\phi_m \frac{\alpha_g\, t_g}{\alpha_d\, t_d}\right)^{7/80} \tag{9}$$

where the superscript m denotes that values are calculated according to measured values, k_s is the Gaucker-Strickler coefficient, S is the bed slope, $G = D_{50}\,(s-1)$ is a quantity related to the mean grain size, D_{50}, and sediment-to-water density ratio, s, θ_s is the critical Shields number for incipient sediment transport and q_s is the dimensionless sediment transport. Values of measured quantities, as well as the threshold values of U_c^m and Fr_c^m calculated by means of Equations 8 and 9, are reported in Table 1. For the sake of clarity, in the calculations we assume the growth period t_g equal to 365 days, according to the hypothesis that, on a yearly timescale, the duration of high flows is much shorter than that of low flows (i.e., $t_d \ll t_g$, see Table 1), as done by Calvani, Perona, Schick, et al. (2019). Additionally, we perform the calculation by accounting for emergent conditions

Table 1
Vegetation Parameters and Hydraulic Data for the River Reaches Involved in the Analysis

River name and reach	α_d [10^{-3} h Km^{-3}]	α_g [cm^2 y^{-1}]	ϕ_m [10^{-3} m^{-2}]	t_d [h]	Y [m]	U_c^m [m s^{-1}]	Fr_c^m [-]
Clearwater 1	3.951	79.94	35.46	1.356	1.72	2.12	0.52
Clearwater 2	3.951	79.94	35.46	1.356	1.93	2.09	0.48
Clearwater 3	3.951	79.94	35.46	1.356	1.93	2.09	0.48
Colorado 1	16.48	38.47	129.3	0.952	0.71	1.60	0.61
Colorado 2	16.48	38.47	129.3	0.952	0.71	1.60	0.61
Colorado 3	16.48	38.47	129.3	0.952	0.71	1.60	0.61
Endrik	16.48	43.84	114.3	0.952	0.82	1.39	0.49
Feshie	16.48	43.84	114.3	0.952	0.46	2.27	1.07
Johnson	2.286	70.64	351.9	1.694	0.87	1.93	0.66
Kander	34.27	233.4	48.35	0.619	0.40	2.00	1.01
Little Snake 1	54.09	147.0	97.4	0.485	1.14	1.49	0.45
Little Snake 2	54.09	147.0	97.4	0.485	1.14	1.50	0.45
NF Clearwater	3.067	163.7	35.11	0.539	0.44	1.66	0.80
Salmon	3.951	309.6	44.14	1.356	1.68	2.50	0.62
San Juan 1	64.35	1.362	50.00	0.395	0.99	2.43	0.78
San Juan 2	64.35	429.5	50.00	0.395	0.99	2.43	0.78
San Juan 3	64.35	291.7	72.59	0.395	1.60	1.72	0.43
San Juan 4	64.35	291.7	72.59	0.395	2.01	2.00	0.45
Selway 1	3.066	166.8	18.4	0.539	0.52	1.21	0.53
Selway 2	3.066	166.8	18.4	0.539	0.53	1.21	0.53
SF Salmon 1	2.286	70.64	351.9	1.694	1.21	2.12	0.62
SF Salmon 2	2.286	70.64	351.9	1.694	1.21	2.12	0.62
Snake 1	0.154	163.7	77.33	1.287	0.61	0.95	0.39
Snake 2	0.154	163.7	77.33	1.287	0.80	0.73	0.26
Virgin	34.27	219.8	95.28	0.619	0.94	2.05	0.68
Wind 1	34.27	41.31	67.27	0.619	0.77	1.94	0.71
Wind 2	34.27	41.31	67.27	0.619	0.76	1.93	0.71
Yampa	16.48	37.53	124.2	0.952	0.95	1.35	0.44
Yellowstone 1	3.951	369.3	15.17	1.356	1.46	1.24	0.33
Yellowstone 2	3.951	375.6	11.56	1.356	1.57	0.91	0.23
Yellowstone 3	3.951	375.6	11.56	1.356	1.27	1.13	0.32
Yellowstone 4	3.951	375.6	11.56	1.356	1.27	1.13	0.32

Note. t_g is 365 days for all the rivers (Calvani, Perona, Schick, et al., 2019).

of the vegetation. This hypothesis allows simplifying plant height, h_v, in Equations 4 and 6, when considering Equations 5 and 7. The comparison between measured (superscript m) and predicted (no superscript) quantities is reported in Figure 3.

Comparison shows that the agreement seems to be satisfactory for both the variables. The correlation coefficient is slightly higher for the critical Froude number (Figure 3a, $R^2 = 0.86$, RMSE = 0.10) than the critical velocity (Figure 3b, $R^2 = 0.80$, RMSE = 0.31 m s^{-1}). Inset panels in Figures 3a and 3b represent the q-q (quantile-quantile) plot of the residuals for threshold velocity and Froude number, respectively (e.g., $U_c - U_c^m$). For each variable, the population of the residuals is compared to a normal distribution $\mathcal{N}$ with the first and second moments

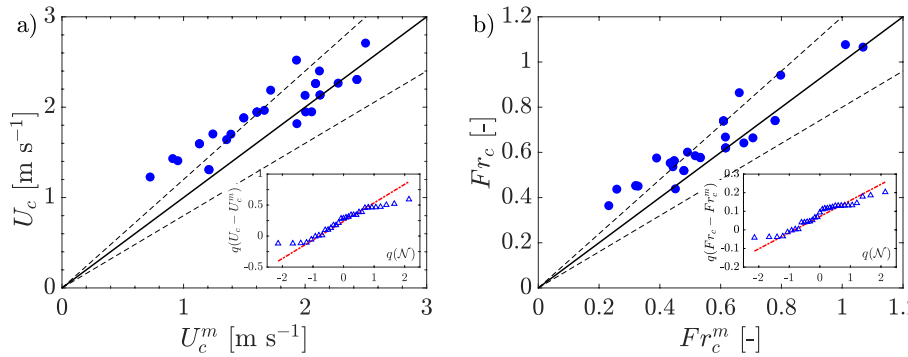

Figure 3. Predicted versus measured critical quantities according to the data in Table 1. Continuous black line is for perfect agreement, dashed lines represent ±20% range. The inset panels show the quantile-quantile plot (*q-q* plot) of the highlighted variable. (a) Comparison and *q-q* plot between predicted, U_c, and measured, U_c^m critical velocity ($R^2 = 0.80$, RMSE = 0.31 m s^{-1}). (b) Comparison and *q-q* plot between predicted, Fr_c, and measured, Fr_c^m critical Froude number ($R^2 = 0.86$, RMSE = 0.10).

(i.e., mean and variance) extracted from the same population. The linear agreement between the two distributions is largely satisfied and this demonstrates that the residuals (i.e., estimating error) are normally distributed for both the variables.

4. Discussion

In this work we provide analytic expressions for the threshold values of hydraulic variables governing the switch between vegetated and barebed conditions in fluvial environments. The analysis is made on the basis of the logistic equation for plant density at equilibrium. In this state, both the temporal and the spatial derivatives cancel out because of stationary and homogeneous conditions. Additionally, the formulations are based on a 1D approach. Surely, this hypothesis introduces simplifications and bias, which can be at the basis of the tendency to slightly overestimate the measured data (Figure 3).

Equation 1 adopts a simple approach to vegetation uprooting based on the decay parameter α_d and the duration t_d. The decay duration, t_d, accounts for the time necessary for the development of scouring processes around plant stems. As a matter of fact, many studies demonstrated that bed erosion may be considered the main responsible of vegetation removal (Bywater-Reyes et al., 2015; Calvani, Francalanci, et al., 2019; Perona et al., 2012), and that flow drag alone is not sufficient for plant uprooting (Type II vs. Type I mechanism according to Edmaier et al., 2011; 2015). As such, while vegetation characteristics of growth (i.e., α_g and ϕ_m) may be obtained just from species properties, determining the decay parameters (i.e., t_d and α_d) requires deeper attention (e.g., Calvani, Perona, Schick, et al., 2019). Alternatively, the presence of scouring processes may be directly introduced in the equation for vegetation dynamics (Equation 1), without significantly alter the main findings of this work. For instance, we may speculate that α_d may be expressed as a function of either the bed level changes or the sediment transport rate, $\vec{q}_s$ (e.g., $\alpha_d = \alpha_d(\nabla \cdot \vec{q}_s)$). However, the hypothesis of equilibrium conditions demands that neither bed level changes may occur over the total timescale T, nor spatial variations of the sediment transport may be accounted for over the considered length-scale.

Both the relationships (Equations 5 and 7) show the presence of the ratio t_g/t_d. This quantity reasonably represents the flow variability because t_g and t_d may be interpreted as the duration of low flow and high flow periods, respectively. The interpretation agrees with the findings of Bertagni et al. (2018) and Calvani, Perona, Zen, et al. (2019) on how flow variability governs the process of vegetation removal. Equation 7 shows a root relationship between the critical Froude number and the carrying capacity, as plotted by Bärenbold et al. (2016) in Figures 9a and 9c (for a comparison, see critical curves in Figure 2b). Moreover, Equation 6 shows that Fr_c does not depend on the width-to-depth ratio β, which was found by Bärenbold et al. (2016) as well in Figures 9b and 9d.

The main properties governing the dynamics of vegetation colonizing riverbed and banks are basically species-dependent (see Table 1 and Calvani, Perona, Schick, et al., 2019). However, these characteristics may vary from a plant to another because of the different growth stage and the growing location (e.g., Tron et al., 2015).

While the proposed relationships may provide results for any values of the vegetation properties, the practical application to real cases deserves special attention. We recall that the hypothesis of equilibrium conditions accounts for the constant value of vegetation characteristics over a timescale longer than the total duration T. Yet, it is worth noting that retrieving data for vegetation properties is time-consuming, and it is usually based on a reach-scale approach (e.g., Forzieri et al., 2011; Latella et al., 2020). Similarly, recent investigations recommend to characterize morphodynamic parameters at a reach-scale length (Carbonari et al., 2020;). Nevertheless, an approach based on a shorter length-scale may be adopted as well, provided that the assessment of vegetation parameters is meaningful to understand the entire channel dynamics.

For a given set of plant properties, both the relationships for threshold values (Equations 4 and 6) show that submerged vegetation is more vulnerable to disturbances induced by flow in comparison to emergent vegetation. For plants in submerged conditions, the proposed relationships predict lower thresholds for higher plants (i.e., older and with a deeper root system). While this seems counter intuitive, as a more robust root system may better resist to removal (Bywater-Reyes et al., 2015; Calvani, Francalanci, et al., 2019), the problem relies in how flow uprooting is modeled in the decay term (Equations 1 and 2). Therein, plant removal depends on the drag exerted by flow velocity (i.e., U^2) on the height of vegetation exposed to flow (i.e., h_v for submerged plants, Y for emergent conditions). Therefore, the higher the submerged height, the lower the flow velocity required for plant removal. Besides, it is supposed that that the decay coefficient is constant throughout the whole life stage, whereas it may assume lower values for older plants, to account for a deeper root system and a reduction in the decay rate.

To our knowledge, no studies specifically provided values of the growth and decay parameters for plants growing under submerged conditions (e.g., macrophytes). At the moment, the quantification of threshold conditions can be assessed by using the proposed equations (Equations 5 and 7) for the plants in emergent conditions for which the growth and decay rates are available (Calvani, Perona, Schick, et al., 2019). Nevertheless, the critical quantities, U_c and Fr_c, can be determined by considering threshold conditions based on different variables. For instance, it is possible to derive the critical flow velocity and Froude number from the stream power per unit width, ω_c. This quantity was previously involved by Bertoldi et al. (2014) to explain the sudden and sharp divide between vegetated and unvegetated conditions occurring in the Magra River (Italy). By involving the Manning equation, it is straightforward to transform the threshold conditions expressed by ω_c into the corresponding values of U_c^m and Fr_c^m, as

$$U_c^m = \omega_c^{2/5}\, k_s^{3/5}\, S^{-1/10} \tag{10}$$

$$Fr_c^m = \omega_c^{1/10}\, k_s^{9/10}\, S^{7/20}\, g^{-1/2} \tag{11}$$

In their work, Bertoldi et al. (2014) found that riparian vegetation disappeared for stream power per unit width in the range $0.046 \le \omega_c \le 0.054$ m^2 s^{-1}, which results in an average value $\omega_c = 0.05$ m^2 s^{-1} $\pm$ 8%. By considering $k_s = 30$ m$^{1/3}$ s^{-1}, and $S = 0.003\,8$ (Bertoldi et al., 2014) in Equations 10 and 11, we obtain $3.92 \le U_c^m \le 4.18\,m\,s^{-1}$ and $0.712 \le Fr_c^m \le 0.724$. These ranges can be summarized as $U_c^m = 4.05$m s^{-1} $\pm$ 3.2% and $Fr_c^m = 0.72 \pm 0.8\%$. While one may have expected that the wide range of threshold conditions given by Bertoldi et al. (2014) would have transformed in a similar range in terms of the critical variables proposed in this work, the existence of a narrower range for critical flow velocity, U_c, and Froude number, Fr_c, supports the existence of a unique threshold value for vegetation (Equations 5–7). Besides the intrinsic scientific significance, the existence of a single threshold condition is of valuable interest for practitioners in the design, for instance, of river restoration projects. To this purpose, both the equations for threshold flow velocity and Froude number regarding vegetation in emergent conditions can be rearranged, by means of the Manning formula. The modified relationships read:

$$U_c^e = \left(\frac{\alpha_g t_g}{\alpha_d t_d}\phi_m\right)^{2/7} k_s^{3/7} S^{3/14} \tag{12}$$

$$Fr_c^e = \left(\frac{\alpha_g t_g}{\alpha_d t_d}\phi_m\right)^{1/14} k_s^{6/7} S^{3/7} g^{-1/2} \tag{13}$$

where the superscript e refers to emergent conditions. Yet, it is worth noting that bed slope, S, and material composition (the roughness parameter, k_s, depends on grain size) play a fundamental role in determining the thresholds for vegetation in emergent conditions. On the contrary, such terms do not appear in the formulation

of the threshold flow velocity, U_c, for submerged plants (see Equations 4 and 5 for comparison). However, plant height, h_v, seems to be crucial to promote vegetation removal and to determine the thresholds for submerged conditions.

5. Conclusions

Herein, the problem of the switch between vegetated and barebed conditions in rivers is mathematically tackled by handling the equation for vegetation dynamics at the steady state. We derive simple formulations for the flow velocity and the corresponding dimensionless Froude number at which the switch may occur. Comparison to data from literature shows that the proposed relationships may capture the fundamentals of the removal process and suggests the existence of a single threshold for which it occurs, rather than a broader range in terms of other variables, such as the stream power. While the thresholds are mainly dependent on vegetation properties, the equilibrium conditions may be affected by climate change and the presence of invasive species. This suggests the hypotheses of vegetation adaptation and species selection by flow regime in fluvial environments. The outcomes have direct implications for practitioners and designers of river restoration projects, where re-naturalization of fluvial systems implies that vegetation may survive in a given flow regime.

Notation

D_{50}	Mean grain size
Fr	Froude number
Fr_c	Threshold Froude number
Fr_c^e	Threshold Froude number for emergent conditions
Fr_c^m	Threshold Froude number from measurements
Fr_v	Threshold Froude number for just submerged vegetation
g	Acceleration due to gravity
G	Parameter relating D_{50} and s
h_v	Vegetation height
k_s	Gauckler-Strickler coefficient
$\mathcal{N}$	Gaussian distribution
q	Quantile
q_s	Dimensionless sediment transport rate per unit width
s	Sediment-to-water density ratio
S	Bed slope
t	Time
T	Total timescale of plant dynamics
t_d	Duration of the decay stage
t_D	Duration of the diffusive stage
t_g	Duration of the growth stage
U	Mean flow velocity
U_c	Threshold flow velocity
U_c^e	Threshold flow velocity for emergent conditions
U_c^m	Threshold flow velocity from measurements
U_v	Threshold flow velocity for submerged vegetation
Y	Water depth
α_d	Decay rate due to flow uprooting
α_g	Growth rate
ϕ	Vegetation density
ϕ_0	Vegetation density at equilibrium
ϕ_m	Carrying capacity
θ_s	Shields number
ω	Stream power
ω_c	Threshold stream power

Data Availability Statement

The full data set reported in Table 1 can be found in Calvani, Perona, Schick, et al. (2019).

Acknowledgments
Authors wish to thank the editor and two anonymous reviewers for their comments and suggestions that greatly improved the manuscript. Open Access Funding provided by Universita degli Studi di Firenze within the CRUI-CARE Agreement.

References

Aberle, J. & Järvelä, J. (2013). Flow resistance of emergent rigid and flexible floodplain vegetation. *Journal of Hydraulic Research*, *51*(1), 33–45. https://doi.org/10.1080/00221686.2012.754795

Bärenbold, F., Crouzy, B., & Perona, P. (2016). Stability analysis of ecomorphodynamic equations. *Water Resources Research*, *52*(2), 1070–1088. https://doi.org/10.1002/2015wr017492

Bendix, J. (1999). Stream power influence on Southern Californian riparian vegetation. *Journal of Vegetation Science*, *10*(2), 243–252. https://doi.org/10.2307/3237145

Bennett, S. J., Pirim, T., & Barkdoll, B. D. (2002). Using simulated emergent vegetation to alter stream flow direction within a straight experimental channel. *Geomorphology*, *44*(1–2), 115–126. https://doi.org/10.1016/s0169-555x(01)00148-9

Bertagni, M. B., Perona, P., & Camporeale, C. (2018). Parametric transitions between bare and vegetated states in water-driven patterns. *Proceedings of the National Academy of Sciences*, *115*(32), 8125–8130. https://doi.org/10.1073/pnas.1721765115

Bertoldi, W., Siviglia, A., Tettamanti, S., Toffolon, M., Vetsch, D., & Francalanci, S. (2014). Modeling vegetation controls on fluvial morphological trajectories. *Geophysical Research Letters*, *41*(20), 7167–7175. https://doi.org/10.1002/2014gl061666

Bywater-Reyes, S., Wilcox, A. C., Stella, J. C., & Lightbody, A. F. (2015). Flow and scour constraints on uprooting of pioneer woody seedlings. *Water Resources Research*, *51*(11), 9190–9206. https://doi.org/10.1002/2014WR016641

Calvani, G., Francalanci, S., & Solari, L. (2019). A physical model for the uprooting of flexible vegetation on river bars. *Journal of Geophysical Research: Earth Surface*, *124*(4), 1018–1034. https://doi.org/10.1029/2018jf004747

Calvani, G., Perona, P., Schick, C., & Solari, L. (2019). Biomorphological scaling laws from convectively accelerated streams. *Earth Surface Processes and Landforms*, *45*(3), 723–735. https://doi.org/10.1002/esp.4735

Calvani, G., Perona, P., Zen, S., Bau', V., & Solari, L. (2019). Return period of vegetation uprooting by flow. *Journal of Hydrology*, *578*. https://doi.org/10.1016/j.jhydrol.2019.124103

Camporeale, C., & Ridolfi, L. (2006). Riparian vegetation distribution induced by river flow variability: A stochastic approach. *Water Resources Research*, *42*(10). https://doi.org/10.1029/2006wr004933

Carbonari, C., Recking, A., & Solari, L. (2020). Morphology, bedload, and sorting process variability in response to lateral confinement: Results from physical models of gravel-bed rivers. *Journal of Geophysical Research: Earth Surface*, *125*(12), e2020JF005773. https://doi.org/10.1029/2020jf005773

Crouzy, B., Bärenbold, F., D'Odorico, P., & Perona, P. (2016). Ecomorphodynamic approaches to river anabranching patterns. *Advances in Water Resources*, *93*, 156–165. https://doi.org/10.1016/j.advwatres.2015.07.011

D'Odorico, P., Laio, F., Porporato, A., Ridolfi, L., & Barbier, N. (2007). Noise-induced vegetation patterns in fire-prone savannas. *Journal of Geophysical Research*, *112*(G2), G02021. https://doi.org/10.1029/2006JG000261

Dosskey, M. G., Vidon, P., Gurwick, N. P., Allan, C. J., Duval, T. P., & Lowrance, R. (2010). The role of riparian vegetation in protecting and improving chemical water quality in streams 1. *JAWRA Journal of the American Water Resources Association*, *46*(2), 261–277. https://doi.org/10.1111/j.1752-1688.2010.00419.x

Edmaier, K., Burlando, P., & Perona, P. (2011). Mechanisms of vegetation uprooting by flow in alluvial non-cohesive sediment. *Hydrology and Earth System Sciences*, *15*(5), 1615–1627. https://doi.org/10.5194/hess-15-1615-2011

Edmaier, K., Crouzy, B., & Perona, P. (2015). Experimental characterization of vegetation uprooting by flow. *Journal of Geophysical Research: Biogeosciences*, *120*(9), 1812–1824. https://doi.org/10.1002/2014jg002898

Forzieri, G., Degetto, M., Righetti, M., Castelli, F., & Preti, F. (2011). Satellite multispectral data for improved floodplain roughness modelling. *Journal of Hydrology*, *407*(1–4), 41–57. https://doi.org/10.1016/j.jhydrol.2011.07.009

Gran, K. B., Tal, M., & Wartman, E. D. (2015). Co-evolution of riparian vegetation and channel dynamics in an aggrading braided river system, Mount Pinatubo, Philippines. *Earth Surface Processes and Landforms*, *40*(8), 1101–1115. https://doi.org/10.1002/esp.3699

Latella, M., Bertagni, M., Vezza, P., & Camporeale, C. (2020). An integrated methodology to study riparian vegetation dynamics: From field data to impact modeling. *Journal of Advances in Modeling Earth Systems*, *12*(8), e2020MS002094. https://doi.org/10.1029/2020ms002094

Lejeune, O., Tlidi, M., & Couteron, P. (2002). Localized vegetation patches: A self-organized response to resource scarcity. *Physical Review E*, *66*(1), 010901. https://doi.org/10.1103/physreve.66.010901

Luhar, M., & Nepf, H. M. (2013). From the blade scale to the reach scale: A characterization of aquatic vegetative drag. *Advances in Water Resources*, *51*, 305–316. https://doi.org/10.1016/j.advwatres.2012.02.002

Nepf, H. M. (2012). Hydrodynamics of vegetated channels. *Journal of Hydraulic Research*, *50*(3), 262–279. https://doi.org/10.1080/00221686.2012.696559

Pasquale, N., Perona, P., Francis, R., & Burlando, P. (2014). Above-ground and below-ground Salix dynamics in response to river processes. *Hydrological Processes*, *28*(20), 5189–5203. https://doi.org/10.1002/hyp.9993

Peirce, S., Ashmore, P., & Leduc, P. (2018). The variability in the morphological active width: Results from physical models of gravel-bed braided rivers. *Earth Surface Processes and Landforms*, *43*(11), 2371–2383. https://doi.org/10.1002/esp.4400

Perona, P., Crouzy, B., McLelland, S., Molnar, P., & Camporeale, C. (2014). Ecomorphodynamics of rivers with converging boundaries. *Earth Surface Processes and Landforms*, *39*(12), 1651–1662. https://doi.org/10.1002/esp.3614

Perona, P., Molnar, P., Crouzy, B., Perucca, E., Jiang, Z., McLelland, S., et al. (2012). Biomass selection by floods and related timescales: Part 1. Experimental observations. *Advances in Water Resources*, *39*, 85–96. https://doi.org/10.1016/j.advwatres.2011.09.016

Schreyers, L., van Emmerik, T., Luan Nguyen, T., Castrop, E., Phung, N.-A., Kieu-Le, T.-C., et al. (2021). Plastic plants: The role of water hyacinths in plastic transport in tropical rivers. *Frontiers in Environmental Science*, *9*, 177. https://doi.org/10.3389/fenvs.2021.686334

Solari, L., Van Oorschot, M., Belletti, B., Hendriks, D., Rinaldi, M., & Vargas-Luna, A. (2016). Advances on modelling riparian vegetation—Hydromorphology interactions. *River Research and Applications*, *32*(2), 164–178. https://doi.org/10.1002/rra.2910

Tron, S., Perona, P., Gorla, L., Schwarz, M., Laio, F., & Ridolfi, L. (2015). The signature of randomness in riparian plant root distributions. *Geophysical Research Letters*, *42*(17), 7098–7106. https://doi.org/10.1002/2015gl064857

Vargas-Luna, A., Crosato, A., & Uijttewaal, W. S. (2015). Effects of vegetation on flow and sediment transport: Comparative analyses and validation of predicting models. *Earth Surface Processes and Landforms*, *40*(2), 157–176. https://doi.org/10.1002/esp.3633

Västilä, K., & Järvelä, J. (2018). Characterizing natural riparian vegetation for modeling of flow and suspended sediment transport. *Journal of Soils and Sediments*, *18*(10), 3114–3130. https://doi.org/10.1007/s11368-017-1776-3

Wang, C., Zheng, S.-s., Wang, P.-f., & Hou, J. (2015). Interactions between vegetation, water flow and sediment transport: A review. *Journal of Hydrodynamics*, *27*(1), 24–37. https://doi.org/10.1016/s1001-6058(15)60453-x

Yang, J., Chung, H., & Nepf, H. (2016). The onset of sediment transport in vegetated channels predicted by turbulent kinetic energy. *Geophysical Research Letters*, *43*(21), 11–261. https://doi.org/10.1002/2016gl071092